NUMERICAL METHODS FOR ACCURATE DESCRIPTION OF ULTRASHORT PULSES IN OPTICAL FIBERS

R. ČIEGIS

Vilnius Gediminas Technical University, Vilnius, Lithuania
e-mail: rc@vgtu.lt

MMK, October 16, 2018

S. Amiranashvili, U. Bandelow, M. Radziunas, R. Čiegis.
Numerical methods for accurate description of ultrashort pulses in optical fibers.
Communications in Nonlinear Science and Numerical Simulation
Vol. 67 (2019) 391–402
https://doi.org/10.1016/j.cnsns.2018.07.031

Grard Mourou
Ecole Polytechnique, Palaiseau, France University of Michigan, Ann Arbor, USA

Donna Strickland
University of Waterloo, Canada

"for their method of generating high-intensity, ultra-short optical pulses"

Optical pulse evolution is described by the one-dimensional reduction of the Maxwell equations

$$\partial_z^2 E - \frac{1}{c^2}\partial_t^2\Big(\hat{\epsilon}E + \hat{\chi}^{(3)}[E,E,E]\Big) = 0. \tag{1}$$

The operators $\hat{\epsilon}$ and $\hat{\chi}^{(3)}$ describe dispersion and nonlinearity, respectively

The frequency-domain representation $\widetilde{E}(z,\omega)$ is related to the field function $E(z,t)$ through

$$\widetilde{E}(z,\omega) = \int_{-\infty}^{\infty} E(z,t) e^{i\omega t} dt, \qquad E(z,t) = \int_{-\infty}^{\infty} \widetilde{E}(z,\omega) e^{-i\omega t} \frac{d\omega}{2\pi}.$$

If the pulse field is decomposed into Fourier harmonics, the action of dispersion operator $\hat{\epsilon}$ is described by

$$\hat{\epsilon} E(z,t) = \int_{-\infty}^{\infty} \epsilon(\omega) \widetilde{E}(z,\omega) e^{-i\omega t} \frac{d\omega}{2\pi}.$$

The mathematical formulation can be gained by using operators related to the refraction index $n(\omega)$ and the wave vector (propagation constant) $\beta(\omega)$, where

$$n(\omega) = \sqrt{\epsilon(\omega)}, \qquad \beta(\omega) = \frac{\omega}{c} n(\omega). \tag{2}$$

Returning to the physical space, we obtain that $F(z, \tau)$ is governed by the FME

$$\partial_z F + \left(\hat{\beta} - V^{-1}\partial_\tau\right) F + \frac{4n_2}{3c}\partial_\tau \left(F^3\right) = 0. \tag{3}$$

The just derived FME is a natural competitor to the GNLSE

$$i\partial_z \psi + \hat{b}\psi + \frac{n_2}{c}(\omega_C + i\partial_\tau)|\psi|^2\psi = 0,$$

$$\hat{b}\psi = \int_{-\infty}^{\infty} b(\Delta)\widetilde{\psi}(z,\Delta)e^{-i\Delta t}\frac{d\Delta}{2\pi},$$

$$b(\Delta) = \beta(\omega_C + \Delta) - \beta_0 - \beta_1\Delta,$$

$$\beta_0 = \beta(\omega_C), \quad \beta_1 = \beta'(\omega_C),$$

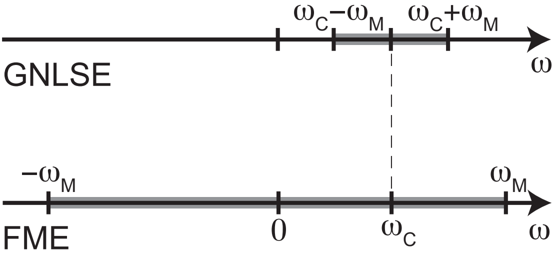

FIGURE : Schematic representation of frequencies resolved by the GNLSE and FME models.

Linear terms in both FME and GNLSE are treated in the frequency domain. We use the following Fourier sum representation of the grid function U_j:

$$U_j = \Big[\mathcal{F}^{-1}(\widehat{U})\Big]_j := \frac{1}{J}\sum_{\ell\in\mathbf{J}} \widehat{U}_\ell e^{-i\omega_\ell jh},\ j \in \mathbf{J}\ = \{-J/2, \dots, J/2-1\},$$

$$\omega_\ell = \frac{\pi\ell}{\tau_R},$$

where $\widehat{U}_\ell$ are the Fourier coefficients defined as

$$\widehat{U}_\ell = [\mathcal{F}(U)]_\ell := \sum_{j\in\mathbf{J}} U_j e^{i\omega_\ell jh}, \quad \ell \in \mathbf{J}. \tag{4}$$

We approximate the FME problem (3) using the following pseudo-spectral symmetric Strang splitting scheme

$$
\begin{aligned}
&\widehat{U}_\ell^{n+\frac{1}{2}} = e^{i\kappa B(\omega_\ell)}\widehat{U}_\ell^n, \quad \ell \in \mathbf{J}, \\
&\frac{U_j^{n+1} - U_j^{n+\frac{1}{2}}}{\kappa} + \frac{4n_2}{3c}\partial_\tau^h\left(\frac{U_j^{n+\frac{1}{2}} + U_j^{n+1}}{2}\right)^3 = 0, \quad j \in \mathbf{J}, \\
&\frac{U_j^{n+\frac{3}{2}} - U_j^{n+1}}{\kappa} + \frac{4n_2}{3c}\partial_\tau^h\left(\frac{U_j^{n+\frac{3}{2}} + U_j^{n+1}}{2}\right)^3 = 0, \quad j \in \mathbf{J}, \\
&\widehat{U}_\ell^{n+2} = e^{i\kappa B(\omega_\ell)}\widehat{U}_\ell^{n+\frac{3}{2}}, \quad \ell \in \mathbf{J}.
\end{aligned}
\tag{5}
$$

The nonlinear advection subproblems can be resolved using the iterative procedure,

$$\frac{\widetilde{U}_j^s - U_j^{n+\frac{r}{2}}}{\kappa} + \frac{4n_2}{3c}\partial_\tau^h\Big(\Big[\frac{\widetilde{U}_j^{s-1} + U_j^{n+\frac{r}{2}}}{2}\Big]^2 \frac{\widetilde{U}_j^s + U_j^{n+\frac{r}{2}}}{2}\Big) = 0, \quad j \in \mathbf{J},$$
$$\widetilde{U}_j^0 = U_j^{n+\frac{r}{2}}, \quad s = 1, \dots, S, \quad r = 1, 2,$$

or can be approximated again by the explicit Richtmyer two-step Lax-Wendroff method:

$$U_{j+\frac{1}{2}}^{n+\frac{r}{4}} = \frac{1}{2}\big(U_j^{n+\frac{r-1}{4}} + U_{j+1}^{n+\frac{r-1}{4}}\big) - \frac{4\kappa n_2}{6hc}\Big(\Big[U_{j+1}^{n+\frac{r-1}{4}}\Big]^3 - \Big[U_j^{n+\frac{r-1}{4}}\Big]^3\Big),$$
$$U_j^{n+\frac{r+1}{4}} = U_j^{n+\frac{r-1}{4}} - \frac{4\kappa n_2}{3hc}\Big(\Big[U_{j+\frac{1}{2}}^{n+\frac{r}{4}}\Big]^3 - \Big[U_{j-\frac{1}{2}}^{n+\frac{r}{4}}\Big]^3\Big), \ j \in \mathbf{J}, \ r = 3, 5.$$

All parallel numerical tests were performed on the computer cluster

"HPC Sauletekis" (`http://www.supercomputing.ff.vu.lt`) at the High-Performance Computing Center of Vilnius University, Faculty of Physics.

We have used nodes with Intel® Xeon® processors E5-2670 with 16 cores (2.60 GHz) and 128 GB of RAM per node. Computational nodes are interconnected via the InfiniBand network.

Let us assume that P processes are used. We decompose the computational grid $\bar{\Omega}_\tau$ and a set of indexes $\mathbf{J}$ into P non-overlapping size-balanced sub-grids Ω_τ^l and subsets $\mathbf{J}_l$, $l = 1, \ldots, P$:

$$\bar{\Omega}_\tau = \bigcup_{l=1}^{P} \Omega_\tau^l, \quad \mathbf{J} = \bigcup_{l=1}^{P} \mathbf{J}_l.$$

1. Solve the local cubic nonlinearity subproblem:

$$U_j^{\tilde{n}+\frac{1}{3}} = \exp\left(i\kappa \frac{n_2}{c}\omega_C |U_j^{\tilde{n}}|^2\right) U_j^{\tilde{n}}, \quad j \in \mathbf{J}_\ell.$$

The algorithm is parallel and no data communication is required.

2. Solve the nonlinear advection subproblem:

$$U_{j+\frac{1}{2}}^{\tilde{n}+\frac{1}{6}} = \frac{1}{2}\left(U_j^{\tilde{n}} + U_{j+1}^{\tilde{n}}\right) - \frac{\kappa n_2}{2hc}\left(\left|U_{j+1}^{\tilde{n}}\right|^2 U_{j+1}^{\tilde{n}} - \left|U_j^{\tilde{n}}\right|^2 U_j^{\tilde{n}}\right),$$
$$U_j^{\tilde{n}+\frac{1}{3}} = U_j^{\tilde{n}} - \frac{\kappa n_2}{hc}\left(\left|U_{j+\frac{1}{2}}^{\tilde{n}+\frac{1}{6}}\right|^2 U_{j+\frac{1}{2}}^{\tilde{n}+\frac{1}{6}} - \left|U_{j-\frac{1}{2}}^{\tilde{n}+\frac{1}{6}}\right|^2 U_{j-\frac{1}{2}}^{\tilde{n}+\frac{1}{6}}\right), \quad j \in \mathbf{J}_\ell.$$

The Richtmyer two-step Lax-Wendroff scheme is explicit, and all computations are done in parallel. The approximation of fluxes requires to exchange values of the solutions at boundaries of subdomains. The communication of data is done only among adjacent processes.

3. Solve the linear propagation subproblem:

$$\widehat{U}_s^{\tilde{n}} = e^{i\kappa b(\omega_s)}\widehat{U}_s^{\tilde{n}}, \quad s \in \mathbf{J}_\ell.$$

This algorithm is implemented in parallel and no communication is required.

The discrete FFT should be done before and after this step, and this transform is the most computation intensive part of the parallel algorithm. It takes about 56% of all CPU time. We have used the parallel version of FFTW library to implement the discrete FFT algorithm.

TABLE : The total wall time T_p, speed-up S_p and efficiency E_p for solving GNLSE problem with two sizes of the discrete problem: small $J = 16384$, $N = 60000$ and large $J = 32768$, $N = 120000$.

$J = 16384,\ N = 60000$	$p = 1$	$p = 2$	$p = 4$	$p = 8$	$p = 16$
T_p	567	327	167	83	48
S_p	1	1.734	3.40	6.83	11.8
E_p	1	0.867	0.850	0.854	0.738
$J = 32768,\ N = 120000$	$p = 1$	$p = 2$	$p = 4$	$p = 8$	$p = 16$
T_p	2280	1300	632	331	188
S_p	1	1.75	3.61	6.89	12.1
E_p	1	0.877	0.902	0.861	0.758

If this parallel algorithm is computed on two nodes with 32 processes, the distributed memory version of the FFTW algorithm is applied.

The efficiency of the parallel algorithm is seriously degraded, the larger problem is solved in $T_{32} = 283$ seconds, which is close to the time used for the same calculations by 8 processes.

In order to show that the parallel efficiency of the remaining part of the algorithm is optimal, computational experiments are done for a larger problem with full nonlinearity but vanishing dispersion. The following results are obtained:

$$T_1 = 1002, \quad T_2 = 504, \quad T_4 = 253, \quad T_8 = 129, \quad T_{16} = 73, \quad T_{32} = 37.$$

Example

Solutions of the FME and GNLSE models are compared. We use $\beta(\omega)$ for bulk fused silica and let the pulse circular frequency ω_C correspond to the wavelength $2.216\,\mu$m $[\nu_0 = \omega_C/(2\pi) = 135.3\,\text{THz}]$.

The initial pulse has a $\cosh^{-1}$ shape and is given by

$$E(z,\tau)|_{z=0} = \underbrace{\frac{\sqrt{P_0}}{\cosh(\tau/\tau_0)}}_{\psi(z,\tau)|_{z=0}} \sin(\omega_C \tau),$$

where $\tau_0 = 13\,\text{fs}$. The seed pulse contains three oscillations of the wave field at half-maximum.

The normalized initial peak power $n_2 P_0 = 0.0288$ is 60% larger than that of the fundamental soliton at frequency ω_C. Such a pulse cannot propagate without changes in its shape, as opposed to fundamental solitons.

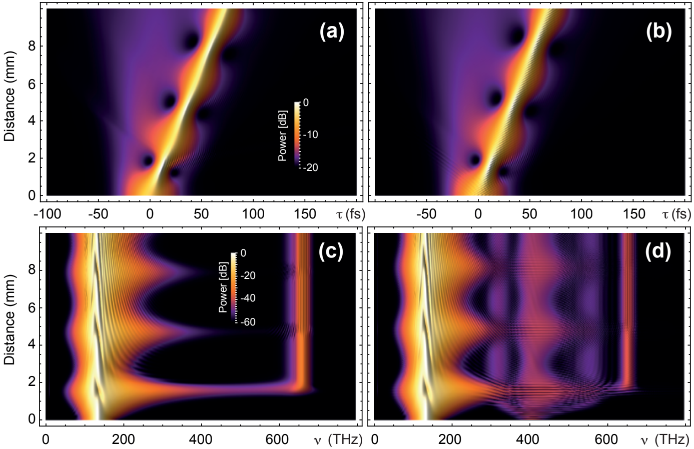

FIGURE : Exemplary solutions of the GNLSE (a,c) and FME (b,d) for a three-cycle pulse that propagates in fused silica. The energy density plots are given in space-time (a,b) and space-frequency (c,d) domains. See text for parameters and discussion.

The GNLSE solution, see Fig. 2(a,c), shows slowly decreasing power oscillations with the increase of z both in space-time [Fig. 2(a)] and space-frequency [Fig. 2(c)] domains.

At maximum compression ($z = 1.5\,\mathrm{mm}$) of the pulse, its spectrum achieves its maximal width, which is sufficient for generation of a wave at the new frequency [650 THz in Fig. 2(c)], the so-called soliton's Cherenkov radiation. The radiation is responsible for asymmetry of the pulse field in Fig. 2(a).

The FME solution is shown in Fig. 2(b,d). The space-time representation is similar to Fig. 2(a), whereas in the frequency domain we see notable differences.

Not only the third harmonic of the carrier frequency becomes visible [at 400 THz in Fig. 2(d)] but also two new Cherenkov-type lines appear.

Such lines attracted recently considerable attention, their adequate explanation and accurate description are still under debate.

A Toolbox of Mathematics

Complex numbers

Hilbert spaces

Hermitian operators

Eigenvalue problems

Fourier transform (FT), ODE theory

Probability theory (mean, or expected value, variance, standard deviation)

Heisenberg's uncertainty principle

$$\Delta X \, \Delta P \geq \frac{\hbar}{2},$$

where X is position, P is linear momentum, $\hbar$ is the Planck constant

$$\hbar = 1.0545718 \cdot 10^{-34}.$$

The Cauchy-Schwarz inequality

$$|(x, y)| \leq \|x\| \, \|y\|.$$

A particle-wave duality and FT.

1. The space of states of a quantum system is not a set, it is a Hilbert linear vector space over complex numbers.

It is composed of elements $|X\rangle$ called ket-vectors or just kets.

Examples of elements:

a) n dimensional column vectors $(x_1, \ldots, x_n)^T, \quad x_j \in \mathbb{C}$;

b) Functions $g(x) \in \mathbb{C}$.

For every ket-vector $|X\rangle$ there is a bra vector in the dual space $\langle X|$.

If z is a complex number, then the bra corresponding to $z\,|X\rangle$ is $\langle X|\, z^*$.

Example:

$$|X\rangle = \begin{pmatrix} x_1 \\ x_2 \\ x_3 \end{pmatrix}, \qquad \langle X| = (x_1^*, x_2^*, x_3^*).$$

The Inner Product

$$\langle X|Y\rangle .$$

The result of this operation is a complex number.

$$\langle Y|X\rangle = \langle X|Y\rangle^* .$$

Examples:

For row and column vectors we define

$$\langle X|Y\rangle = \left(x_1^*, x_2^*, x_3^*\right) \begin{pmatrix} y_1 \\ y_2 \\ y_3 \end{pmatrix},$$

for bras and kets defined as functions:

$$\langle G|H\rangle = \int_a^b g^*(x)h(x)dx.$$

Orthonormal Basis

$$|A\rangle = \sum_j \alpha_j |j\rangle ,$$

where the orthonormal basis of ket-vectors is used

$$\begin{aligned} \langle j|j\rangle &= 1, \quad j = 1, \dots, N, \\ \langle j|k\rangle &= 0, \quad j, k = 1, \dots, N, \;\; j \neq k. \end{aligned}$$

Coefficients are computed as

$$\alpha_j = \langle j|A\rangle ,$$

then we can rewrite the formula as

$$|A\rangle = \sum_j |j\rangle \langle j|A\rangle .$$

2. Observables are represented by Hermitian linear operators.

Observables are also associated with a vector space!

Linear Operators

Let us denote linear operators $\mathbf{M}: \ H \to H$:

$$\mathbf{M} \left| X \right\rangle = \left| Y \right\rangle, \quad \left| X \right\rangle, \left| Y \right\rangle \in H.$$

Hermitian linear operators:

1. Conjugate operators:

$$\mathbf{M} \left| X \right\rangle = \left| Y \right\rangle, \quad \left\langle X \right| \mathbf{M}^{\dagger} = \left\langle Y \right|, \quad \mathbf{M}^{\dagger} = (\mathbf{M}^{\mathbf{T}})^{*}.$$

2.

$$\mathbf{M} = \mathbf{M}^{\dagger}.$$

1. Eigenvalues of Hermitian operators are real:

$$\mathbf{L} \left|\lambda\right\rangle = \lambda \left|\lambda\right\rangle, \quad \lambda \in \mathbb{R}.$$

2. The eigenvectors of a Hermitian operator are defining a complete set.

3. If λ_1 and λ_2 are two unequal eigenvalues of a Hermitian operator, then the corresponding eigenvectors are orthogonal.

The possible results of a measurement are the eigenvalues of the operator that represents the observable.

4. If $|A\rangle$ is the state-vector of a system, and the observable $\mathbf{L}$ is measured, the probability to observe value λ_k is

$$P(\lambda_k) = |\alpha_k|^2$$

where

$$|A\rangle = \sum_j \alpha_j \, |\lambda_j\rangle \, .$$

After the measurement the state vector $|A\rangle = |\lambda_k\rangle$.

For kets-functions we get the probability density

$$P(x) = \psi^*(x)\psi(x),$$

and the probability is given by the integral

$$P(a, b) = \int_a^b P(x)dx = \int_a^b \psi^*(x)\psi(x)dx.$$

The expectation value of observable $\mathbf{L}$ for a given state $|\Psi\rangle$ is the average

$$\langle \mathbf{L} \rangle := \langle \Psi | \mathbf{L} | \Psi \rangle = \sum_{\alpha} \alpha P(\alpha).$$

$$\bar{\mathbf{L}} = \mathbf{L} - \langle L \rangle \, \mathbf{I}.$$

The uncertainty (or standard deviation) of $\mathbf{L}$ is defined by

$$(\Delta \mathbf{L})^2 = \langle \Psi | \bar{\mathbf{L}}^2 | \Psi \rangle = \sum_{\alpha} \bar{\alpha}^2 P(\alpha).$$

Let $|X\rangle$ and $|Y\rangle$ be any two vectors in a complex vector space, then

$$2\sqrt{\langle X|X\rangle}\sqrt{\langle Y|Y\rangle} \geq |\langle X|Y\rangle + \langle Y|X\rangle| \,.$$

Let $\mathbf{A}$ and $\mathbf{B}$ be any two observables, we define

$$|X\rangle = \bar{\mathbf{A}}\,|\Psi\rangle\,, \quad |Y\rangle = i\bar{\mathbf{B}}\,|\Psi\rangle\,.$$

Then we get from C-S inequality

$$\begin{aligned} 2\sqrt{\langle\bar{\mathbf{A}}^2\rangle}\sqrt{\langle\bar{\mathbf{B}}^2\rangle} &\geq \left|\langle\Psi|\bar{\mathbf{A}}\bar{\mathbf{B}}|\Psi\rangle - \langle\Psi|\bar{\mathbf{B}}\bar{\mathbf{A}}|\Psi\rangle\right| \\ &\geq |\langle\Psi|[\mathbf{A},\mathbf{B}]|\Psi\rangle|\,, \quad [\mathbf{A},\mathbf{B}] = \mathbf{AB} - \mathbf{BA}. \end{aligned}$$

since $[\mathbf{A},\mathbf{B}] = [\bar{\mathbf{A}},\bar{\mathbf{B}}]$.

$$\Delta \mathbf{A}\, \Delta \mathbf{B} \geq \frac{1}{2} \left| \langle \Psi | [\mathbf{A}, \mathbf{B}] | \Psi \rangle \right| ,$$

We know the state of the particle $|\Psi\rangle$ on x-axis.
We want to measure the position x and the momentum p.

The position operator $\mathbf{X}$ is defined by

$$\mathbf{X} |\Psi\rangle = x\psi(x).$$

We solve the eigenvalue problem

$$\mathbf{X}\,|\Psi\rangle = x_0\,|\Psi\rangle\,, \quad x_0 \in \mathbb{R}.$$

Every real number x_0 is an eigenvalue of $\mathbf{X}$ and the corresponding eigenvectors are the Dirac delta functions:

$$|x_0\rangle = \delta(x - x_0).$$

Our particle is a real PARTICLE with the wave function equal to the state-vector

$$\langle x|\Psi\rangle = \psi(x).$$

The momentum operator **P** is defined by

$$\mathbf{P}\psi(x) = -i\hbar\frac{d\psi(x)}{dx}.$$

Next solve the eigenvalue problem (ODE problem)

$$\mathbf{P}\left|\Psi\right\rangle = p\left|\Psi\right\rangle.$$

The eigenvalue is any real value p, the corresponding eigenfunction

$$|p\rangle = \frac{1}{\sqrt{2\pi}}e^{ipx/\hbar}.$$

Our particle looks like a WAVE (FT relation)

$$\langle p|\Psi\rangle := \widetilde{\psi}(p) = \frac{1}{\sqrt{2\pi}}\int_{-\infty}^{\infty} e^{ipx/\hbar}\psi(x)dx.$$

Compute product **XP**

$$\mathbf{XP}\psi(x) = -i\hbar x \frac{d\psi(x)}{dx}.$$

Now compute **PX**

$$\mathbf{PX}\psi(x) = -i\hbar x \frac{d\psi(x)}{dx} - i\hbar\psi(x).$$

Thus the commutator acts as:

$$[\mathbf{X}, \mathbf{P}]\psi(x) = i\hbar\psi(x).$$

Heisenberg's estimate

$$\Delta\mathbf{X}\,\Delta\mathbf{P} \geq \frac{1}{2}\left|i\hbar\,\langle\Psi|\Psi\rangle\right| = \frac{\hbar}{2}.$$